Contents lists available at ScienceDirect

# Colloids and Surfaces B: Biointerfaces

journal homepage: www.elsevier.com/locate/colsurfb

# Synthesis and characterization of antimicrobial colloidal polyanilines

Ajay Jose [a], Mahima Bansal [b], Darren Svirskis [b], Simon Swift [a], Marija R. Gizdavic-Nikolaidis [a,c,*]

[a] Department of Molecular Medicine and Pathology, School of Medical Sciences, the University of Auckland, Auckland 1023, New Zealand
[b] School of Pharmacy, the University of Auckland, Auckland 1023, New Zealand
[c] University of Belgrade, Vinča Institute of Nuclear Sciences, National Institute of the Republic of Serbia, P. O. Box 522, Belgrade 11001, Serbia

## ARTICLE INFO

## ABSTRACT

The potential application of colloidal polyaniline (PANI) as an antimicrobial is limited by challenges related to solubility in common organic solvents, scalability, and antimicrobial potency. To address these limitations, we introduced a functionalized PANI (fPANI) with carboxyl groups through the polymerisation of aniline and 3-aminobenzoic acid in a 1:1 molar ratio. fPANI is more soluble than PANI which was determined using a qualitative study. We further enhanced the solubility and antimicrobial activity of fPANI by incorporating Ag nanoparticles onto the synthesized fPANI colloid via direct addition of 10 mM AgNO$_3$. The improved solubility can be attributed to an approximately 3-fold reduction in size of particles. Mean particle sizes are measured at 1322 nm for fPANI colloid and 473 nm for fPANI-Ag colloid, showing a high dispersion and deagglomeration effect from Ag nanoparticles. Antimicrobial tests demonstrated that fPANI-Ag colloids exhibited superior potency against Gram-positive *Staphylococcus aureus*, Gram-negative *Escherichia coli*, and Bacteriophage PhiX 174 when compared to fPANI alone. The minimum bactericidal concentration (MBC) and minimum virucidal concentration (MVC) values were halved for fPANI-Ag compared to fPANI colloid and attributed to the combination of Ag nanoparticles with the fPANI polymer. The antimicrobial fPANI-Ag colloid presented in this study shows promising results, and further exploration into scale-up can be pursued for potential biomedical applications.

## 1. Introduction

The conducting polymer (CP) polyaniline (PANI) has been extensively studied and applied for tissue engineering scaffolds, controlled drug delivery systems, biosensors and antimicrobial applications [1]. Additionally, the demand to combat antibiotic resistance and viral pandemics in hospitals has driven research into antimicrobial agents like PANI for use as biocidal coating additives, limiting microbial transmission through surfaces [2–8]. PANI is an attractive option for these applications because its simple and relatively low-cost synthesis produces a polymer with high electrical conductivity in doped states, biocompatibility, unique redox properties, and good thermal, chemical, and environmental stability [9].

However, the use of PANI is restricted to a certain extent due to the insolubility of the polymer in common laboratory solvents, which strongly influences its processability and scalability [10,11]. To overcome this problem, several methodologies have been proposed [12–14], with the most successful and scalable method of producing processible PANI material for biomedical applications being the production of functionalized derivatives of PANI in aqueous colloidal dispersion form [15–17].

Aqueous colloidal dispersions of PANI can be efficiently produced by a "Rapidly Mixed" reaction method [18,19]. Conventionally, aniline is polymerised in situ while a steric stabiliser stops the macroscopic precipitation of PANI during polymerisation, giving a stable colloidal dispersion. A range of water-soluble polymers and inorganic colloids, including polyvinylpyrrolidone (PVP), have been utilized to stabilize PANI dispersions [19–21], with PVP being particularly favoured due to its high resistance to acidic pH and soluble ions [19,21].

With the aim of creating a soluble form of PANI, Gizdavic-Nikolaidis et al. carried out a synthetic method where aniline is co-polymerised with its derivate 3-amino benzoic acid (3ABA), giving a functionalized PANI (fPANI) [22–24]. Although fPANI has lower conductivity ~10$^{-1}$ fold than PANI, it is soluble in common solvents [10,11,15,22,24,25] and has better antimicrobial activity, thereby increasing the potential of fPANI material use in biomedical applications [22,24]. In this study, we used PVP to make colloids of fPANI in acidic medium.

The use of colloid fPANI in conjunction with Ag has not been

explored in literature, which serves as a research gap in the field. Several papers have reported that tethering of Ag nanoparticles into PANI matrix provides the CP composite with both enhanced antibacterial activity and conductivity in comparison to PANI [26–35]. Therefore, we hypothesise that Ag will also enhance the properties of fPANI and boost its antimicrobial properties. Even though the concept of antiviral polymers has been proposed [6], the descriptions of the antiviral properties of PANI or fPANI are only demonstrated against enveloped Vaccinia virus [7]. Therefore, the antiviral efficacies for PANI and fPANI may need to be further extended to other viral strains. One of the simplest virus surrogates, bacteriophages are viruses that infect and replicate in bacterial cells, making them easier to handle and replicate for antiviral studies. For example, bacteriophage Phi X174 is a non-enveloped virus that infects *E. coli* and has been utilized as a model for the study of disinfection processes used to prevent fomite-mediated transmission [4] and in water treatment [5], where its simple cultivation and safely for humans is an advantage [2,3].

In this study, we test the hypothesis that PANI and fPANI colloids produced with Ag nanoparticles will have enhanced antimicrobial activity. We report a facile approach of preparing PANI and fPANI colloids with Ag nanoparticles in a one-pot synthesis approach. Morphology, structural and optical properties of PANI (as a control), fPANI, PANI-Ag and fPANI-Ag colloids are evaluated. The antibacterial activity of all colloids was assessed against representative Gram-negative (*E. coli*) and Gram-positive (*S. aureus*) bacteria, while the antiviral activity against bacteriophage PhiX 174 is reported. We demonstrate enhanced chemical and antimicrobial properties of PANI-Ag and fPANI-Ag colloids in comparison to pure PANI and fPANI, and discuss new possibilities for applications for fPANI-Ag colloids.

## 2. Materials and methods

### 2.1. Materials

Aniline (ACS reagent $\geq$ 99.5%), 3-aminobenzoic acid, 3ABA (98%), hydrochloric acid, HCl (ACS reagent, 37%), polyvinylpyrrolidone, ethanol, EtOH (ACS reagent $\geq$ 99.5%), PVP 360 (number average molecular weight Mn 360k Da), ammonium persulfate, $(NH_4)_2S_2O_8$ (ACS reagent, $\geq$98.0%) and silver nitrate, $AgNO_3$ (ACS reagent, $\geq$99.0%) were obtained from Sigma Aldrich. Sodium borohydride, $NaBH_4$ ($\geq$98%) was purchased from VWR International.

Microbiological media Difco Tryptic Soy Broth, Difco Nutrient Broth and Difco bacteriological agar and Lab M NaCl were purchased from Fort Richard Laboratories. All microorganisms were acquired from the American Type Culture Collection (ATCC). The bacterial test strains studied were *S. aureus* ATCC 6538 and *E. coli* ATCC 25922. Antiviral studies were performed Bacteriophage Phi X174 ATCC 13706-B1 and its host for propagation was *E. coli* ATCC 13706.

### 2.2. Synthesis

#### 2.2.1. Synthesis of PANI and fPANI colloids

To prepare a PANI dispersion in PVP using an in-situ polymerization method, PVP (2.0 g) was dissolved in 50 mL of 1 M HCl by mechanical stirring, followed by addition of aniline (4 mL). $(NH_4)_2S_2O_8$ (4.8 g) was dissolved in 50 mL of 1 M HCl. $(NH_4)_2S_2O_8$ solution was added dropwise to the aniline solution under mechanical stirring and the reaction mixture was kept overnight under mechanical stirring [19,21]. The monomer to oxidant ratio was kept constant as it was used in rapid-mixing reaction method. The resultant colloids were centrifuged, and then they were washed with water three times and re-dispersed in 50 mL water. In order to prepare fPANI dispersion the method as above was followed with additional aniline (1.62 mL) and its derivate 3ABA (2.43 g) [22].

In order to prepare PANI/fPANI with Ag nanoparticles, we added 1.5 mL of 10 mM $AgNO_3$ into 50 mL of PANI or fPANI colloid dropwise

and stir for 24 h [36]. After 24 h PANI or fPANI colloid was centrifuged. The product was washed using MQ water (three times) and resuspend as colloid in 50 mL water.

As a control we prepared Ag nanoparticles colloid by adding 1.5 mL of 10 mM $AgNO_3$ dropwise to 50 mL of 20 mM $NaBH_4$ solution containing 2.0% (w/v) PVP in an ice bath and stirred the solution until the colloid become yellow color [37]. The resultant Ag nanoparticles colloid was stored at 4 °C.

### 2.3. Characterization

#### 2.3.1. Solubility test

A qualitative study was conducted to test the solubility of samples in a common solvent, ethanol [38]. For this study, around 10 mg of the colloid was added separately to 2 mL of ethanol with stirring. More solvent was added at a rate of 1 mL every 10 min until reaching a total volume of 10 mL. The test is purely qualitative, with the transparency of the resulting solution serving as the solubility criteria. If the solution is clear and transparent, it is considered soluble. However, if it appears thick, turbid, with visible particles settling down, it is deemed poorly or sparingly soluble. If no color change is observed in the ethanol solution, it is termed as insoluble [38].

#### 2.3.2. Dynamic light scattering (DLS)

This technique is used to determine the average particle size of colloids. Since the colloid samples obtained after the synthesis step are highly concentrated, the colloid samples were diluted 60 times in 1 M HCl [21]. The colloidal properties, such as particle size, zeta potential, and polydispersity of these diluted colloids, were analyzed using Malvern Panalytical ZetaSizer Nano ZS. The pH of the samples was recorded along with the above mentioned properties.

#### 2.3.3. Scanning Electron Microscopy (SEM)

SEM was used to obtain information regarding the surface morphology and individual particle size of the colloid samples. The colloid samples were diluted 60 times in 1 M HCl and 200 μL of this diluted colloid was drop casted onto a glass coupon. The liquid phase was allowed to vaporize at room temperature inside a fume hood. Afterwards, the dried colloidal samples were sputter coating using Hitachi E-1045 ion sputter for 60 s, and the sample was coated at room temperature with Platinum (10 nm thickness of Pt). The SEM analysis was carried out using Hitachi SU-70 Schottky field emission scanning electron microscope. For particle size measurements, five measurements for each sample were taken at randomly selected locations of the SEM micrograph.

#### 2.3.4. Fourier Transform Infrared (FTIR) spectroscopy

The chemical structures of PANI and fPANI samples were characterized using FTIR measurements. This technique enabled the observation of any shifts in the peaks, indicating interactions between Ag nanoparticles and the conducting polymer. The spectra was acquired using Bruker VERTEX 70 FT-IR Spectrometer in range of 400–4000 cm$^{-1}$ with 100 scans. The colloid samples of PANI and fPANI were dried at room temperature. The dried samples were then separated into particles, which were uniformly dispersed in potassium bromide (KBr) and compressed into pellets for FTIR measurements.

#### 2.3.5. Ultraviolet–visible light (UV-Vis) spectroscopy

The absorbance spectra were recorded to analyse the electronic transitions of PANI and fPANI particles in the colloids, focusing on the influence of Ag on these properties. The colloid samples were diluted 60 times in 1 M HCl and the UV-Vis spectrum was recorded using Shimadzu UV-2600 spectrophotometer using a quartz cuvette in the range of 200–800 nm.

### 2.3.6. Cyclic Voltammetry (CV) and Electrochemical Impedance Spectroscopy (EIS)

The purpose of conducting cyclic voltammetry (CV) and electrochemical impedance spectroscopy (EIS) studies for polymers is to characterize their electrochemical properties and behavior. In order to facilitate electrochemical measurements, the unmodified PANI, fPANI and their PANI/fPANI-Ag colloids were converted into a stable film form. The use of film as working electrodes offers advantages such as ease of handling and improved surface area to volume ratio [39]. To prepare the films, a binder solution was created by mixing hydroxypropyl methylcellulose (HPMC) and polyvinyl alcohol (PVA) in a 1:1 ratio. Both polymers were used at a concentration of 5% (w/v). The choice of HPMC and PVA was guided by their non-conductive nature, thereby ensuring that the measured electrochemical properties are intrinsic to the PANI, fPANI, and their PANI/fPANI-Ag colloids. Following the preparation of binder solution, the colloidal samples were added in a 1:1 ratio to the binder mixture. The mixture was sonicated for 5 min to allow the formation of uniform dispersion of PANI and fPANI colloids. The films were casted onto the glass Petri dishes, and allowed to dry at room temperature for 24 h to ensure complete solvent evaporation and film formation.

The electrochemical properties of PANI, fPANI and their PANI/fPANI-Ag colloids were determined using a Biologic VSP-300 multichannel potentiostat. A three-electrode cell was assembled using PANI, fPANI or PANI/fPANI-Ag colloids as working electrode, Ag/AgCl reference electrode and platinum (Pt) mesh as counter electrode. A 0.01 M phosphate buffer saline (PBS) served as electrolyte solution. A 0.01 M phosphate-buffered saline (PBS) solution served as the electrolyte [40]. The impedance of all coatings was measured by EIS, a sinusoidal excitation signal with an amplitude of 10 mV was applied over a range of 1 Hz to 100 kHz [40], and measurements were taken at 9 points per decade (on a logarithmic scale). This frequency range was selected to obtain both the high frequency charge transfer and low frequency diffusion process relevant to PANI's electrochemical behavior. A Nyquist plot of EIS measurement of each sample was prepared to calculate the impedance magnitude ($|Z|$). For CV measurements, the voltage was scanned from $-1.5$ V to $+0.5$ V at a rate of 50 mV/s, a range chosen based on preliminary experiments and literature to ensure capture of all relevant redox processes [41].

### 2.3.7. Inductively coupled plasma mass spectrometry (ICP-MS) spectroscopy

The concentration of Ag in the samples was evaluated using the Agilent 7700 Inductively Coupled Plasma Mass Spectrometry (ICP-MS) technique. This enabled us to determine the amount of Ag present in the colloid samples PANI-Ag and fPANI-Ag. Additionally, it allowed us to prepare Ag nanoparticle colloids with the same concentration, which was also confirmed by ICP-MS. This standardization was crucial for obtaining comparative antimicrobial data between Ag nanoparticles, PANI-Ag and fPANI-Ag. Prior to ICP-MS analysis, the colloid samples were diluted 400 times in a 50 mL centrifuge tube using the diluent containing 10% v/v HCl and 3.5% v/v $HNO_3$ [42].

### 2.4. Antimicrobial studies

Antimicrobial activity of the colloids was evaluated through testing their ability to kill bacteria (bactericidal) or inactivate viruses (virucidal). The minimum bactericidal concentration (MBC) was determined for *E. coli* and *S. aureus* using the method previously described by Gizdavic-Nikolaidis et al. [8,35].

Minimum virucidal concentration (MVC) of the prepared colloids was determined for the bacteriophage PhiX 174. A preparation of PhiX 174 was prepared according to ATCC instructions with a suspension of $\sim 10^8$ plaque forming units (PFU)/mL obtained. To determine MVC, the colloids were diluted to generate replicate 1 mL suspensions in Nutrient Broth (NB) containing 0.5% w/v sodium chloride, NaCl (NB/NaCl) at 2,

1, 0.5, 0.25, 0.125, 0.06, 0.03 and 0 wt%. An inoculum of 1 mL of bacteriophage suspension at $10^6$ PFU/mL in NB/NaCl was added to each colloidal sample and incubated for 24 h at 37 °C with shaking at 200 rpm. After 24 h, the suspension was filtered through a 0.2 μm filter (polyethersulfone membrane, Thermo Scientific) to remove colloidal PANI or fPANI particles from the bacteriophage. The bacteriophage has a diameter of $\approx 25$ nm [43] and will pass through the filter membrane. 100 μL of the filtrate was added to 100 μL of $10^7$ colony forming units (CFU)/mL of bacteriophage propagation host and the bacteriophage-host suspension was incubated for 15 min at room temperature to allow infection of the host bacterium. The infected host suspension (200 μL) was transferred to 3 mL molten soft agar (NB/NaCl + 0.5% w/v agar) and poured onto a pre-warmed nutrient agar plate. All plates were incubated at 37 °C overnight and plaques counted the next day. The MVC was taken as the minimum concentration of sample that gave at least a 1000-fold reduction in viable virus after 24 h contact with the sample, measured in practice as less than 10 PFU on the recovery plate.

## 3. Results and discussion

### 3.1. Solubility, DLS and Zeta potential analyses

The qualitative solubility test showed that PANI-Ag and fPANI-Ag were more soluble than their pure forms (supplementary data Fig. S1). This preliminary study shows that the solubility in ethanol of samples follows the order fPANI-Ag> PANI-Ag> fPANI> PANI. The hypothesis that fPANI is more soluble than PANI is well supported by this study. The increase in solubility observed in samples incorporating Ag can be attributed to the reduction in particle size, as elaborated in the subsequent sections and discussions.

The colloids were characterised by DLS to determine particle size and polydispersity, as well as zeta potential (Table 1). All colloids remain stable even though zeta potential is lower ($< \pm 3.0$ mV) than expected. Stability may be attributed to the PVP present in the colloidal system. Addition of Ag nanoparticles reduces the particles size of the colloid. This result suggests that Ag ions acting as dopants for PANI and fPANI system preventing coalescence of polymer particles [44]. Addition of Ag ions into the PANI and fPANI colloids may lead to interchain separation due to the large size of the dopant, which acts against the polymer chains' ordering and closure [45]. The observed particle size difference is explained in detail in Section 3.2 below, where we compared the particle size analysis using SEM.

Table 1

Others have reported spherical PANI particles with hydrodynamic diameter in the range 300–600 nm prepared using PVP 70,000 MW as a steric stabiliser [46]. We attribute the colloid stability to steric interactions and not electrostatic interactions. Typically, to electrostatically stabilise a colloidal dispersion the zeta potential are higher than $\pm$ 30 mV [47,48].

**Table 1**

Concentration of Ag, particle size, PDI and zeta potential of colloidal samples.

| Samples | Amount of Ag * (μg/mL) | Particle size (nm) | PDI | Zeta potential (mV) | pH |
|---|---|---|---|---|---|
| PANI | - | 791.1 ± 9.6 | 0.337 ± 0.02 | +3.89 ± 0.23 | 3.52 |
| fPANI | - | 1322.3 ± 40.7 | 0.274 ± 0.05 | -0.842 ± 0.03 | 3.12 |
| PANI-Ag | 82.86 ± 0.86 | 320.5 ± 27.6 | 0.353 ± 0.02 | -0.652 ± 0.01 | 3.80 |
| fPANI-Ag | 82.50 ± 0.17 | 472.5 ± 49.8 | 0.254 ± 0.07 | -1.11 ± 0.05 | 3.30 |
| Ag | 95.55 ± 0.49 | 113.5 ± 2.2 | 0.661 ± 0.05 | +31.70± 1.31 | 10.24 |

* The amount of Ag is calculated in the total volume of the colloid.

The concentration of Ag in the colloidal system (PANI-Ag and fPANI-Ag) was found be around 100 μg mL$^{-1}$. We speculate that in combination with PANI or fPANI this amount of Ag can act in synergy to boost the biocidal activity of PANI and fPANI. Even though it is possible to add more Ag, it was observed that any amount beyond 100 μg/mL could disrupt the stability of the colloid leading to agglomeration and precipitation of particles [49].

*3.2. SEM*

In Fig. 1 SEM micrographs show the spherical morphology for PANI and fibre-like morphology for fPANI with an approximate diameter of less than 100 nm. The spherical structure of PANI colloid may also be due to the effect of PVP present in the polymerising medium [24]. For both PANI-Ag and fPANI-AgNP colloids (Fig. 1c and d) we noticed that Ag nanoparticles are incorporated into the polymer matrix as previously reported [24]. This is in agreement with structural changes observed after incorporation Ag nanoparticles in FTIR spectra of PANI-Ag and fPANI-Ag colloids. The sizes of individual particles of all samples were measured using SEM technique (supplementary data Fig. S2).

We observed a difference between the dimensions extracted from DLS (Table 1) and SEM (supplementary data Fig. S2 and Table S1). DLS provides an average size of particles in the colloid system, whereas particle size analysis using SEM was conducted on dried samples. Naturally, this variance in sample preparation leads to discrepancies in values. It should be noted that the measured particle dimensions might be affected by shrinking during sample preparation for SEM [50]. Furthermore, in colloid form, agglomerates of individual particles of PANI, fPANI, PANI-Ag, and fPANI-Ag particles exist due to the presence of PVP rather than isolated particles in the colloid samples [19,21]. The presence of PVP leads to stable PANI agglomerate, which gives a higher particle size with DLS [19,21].

On the other hand, SEM micrographs aid in distinguishing and marking individual particles of the agglomerates more effectively due to their magnification and high resolution [50]. Therefore, DLS records a higher value for particle size depending on the chemical interaction between the polymers or nanoparticles present in the colloid and SEM gives relatively less size values for the same sample [19,21,50]. Despite these differences, the trend in size disparities between samples analysed with DLS and SEM remains consistent for PANI and PANI-Ag and for fPANI and fPANI-Ag colloid (Fig S2a-d).

The SEM micrographs (Fig. S2a) reveal the individual PANI particle size to be 61.9 nm. Furthermore, each particle, with a diameter of 61.9 nm, forms agglomerates, with the size measured at 791.1 nm using DLS (Table S1).The agglomerate size of fPANI obtained from DLS study is relatively higher than that of PANI (Table S1). This can be attributed to the increased level of interaction between the carboxyl groups of fPANI and the carbonyl groups of PVP, resulting in a greater degree of agglomeration [51]. Incorporation of Ag reduces the size of PANI agglomerates from 791.1 nm to 320.5 nm for PANI-Ag, and from 1322.3 nm to 472.5 nm for fPANI to fPANI-Ag. This reduction may be attributed to the dispersion of PANI agglomerates by Ag. Possible reasons for this deagglomeration upon Ag addition include physical stirring for 24 h and electrostatic interactions between Ag ions and PANI polymer, leading to deagglomeration [44,52]. Ultimately, smaller PANI-Ag agglomerates are stabilized by PVP in the colloid system [52]. Comparing the size values between PANI and fPANI from SEM, we observe that the individual PANI particle size was found to be 61.9 nm, which is lower than the corresponding value for fPANI, which is 162.0 nm. As observed with DLS measurements, the increase in fPANI and PVP interaction may have contributed to the increase in particle size [51]. As observed with DLS measurements, the increase in fPANI and PVP interaction may have contributed to the increase in particle size [51]. With the addition of Ag, the size of PANI particles increases from 61.9 nm to 108.4 nm for PANI-Ag and from 162.0 nm to 205.6 nm for fPANI to fPANI-Ag. As Ag becomes incorporated onto individual PANI particles, it thereby increases the size of PANI in the PANI-Ag system [53]. The difference in the increase of particle size from PANI to PANI-Ag and fPANI to fPANI-Ag derivatives is speculated to be due to Ag particles being more dispersed in the fPANI matrix than being attached to each fPANI particle. The interaction of Ag with PANI and fPANI is different due to the presence of the -COOH functionality in fPANI [54].
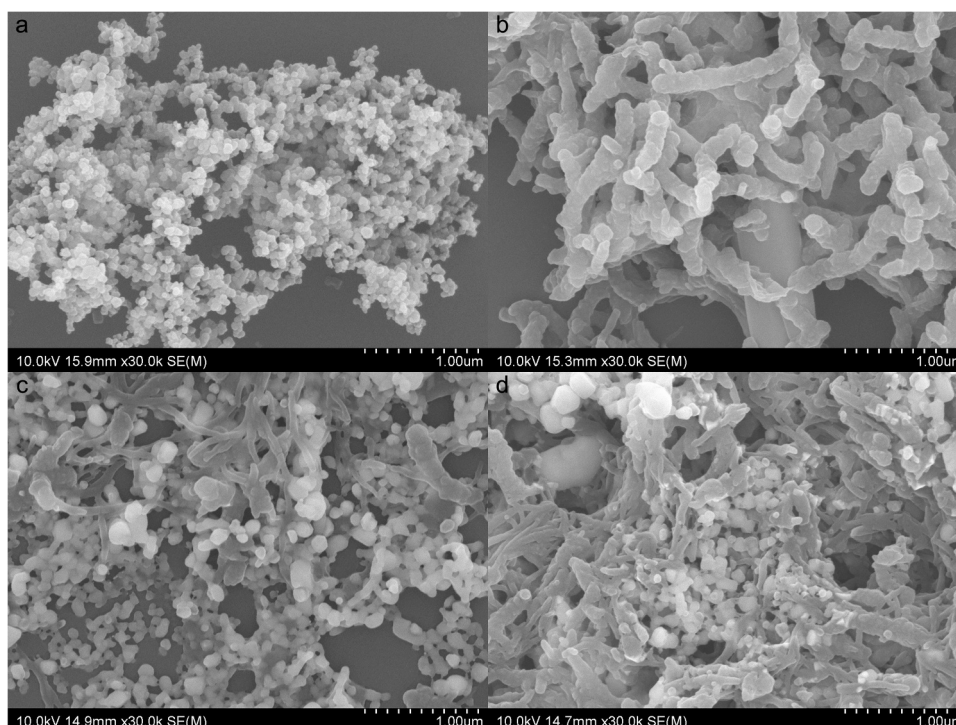


**Fig. 1.** SEM micrographs of a) PANI, b) fPANI, c) PANI-Ag and d) fPANI-Ag.

*3.3. FTIR spectroscopy*

The FTIR spectra of PANI and fPANI, and PANI-Ag and fPANI-Ag colloids are presented in Fig. 2. For PANI colloid (Fig. 2a), we observed all key PANI peaks as previously reported [15,35,55,56]: N−H stretching vibration at 3136 cm$^{-1}$, C−C quinoid ring stretching peak at 1566 cm$^{-1}$, C−C benzenoid ring stretching band at 1405 cm$^{-1}$, C=N band of imine group at 1304 cm$^{-1}$, electronic band of PANI at 1181 cm$^{-1}$ and C−H out-of-plane bending in 1,4-disubstituted ring structures at 804 cm$^{-1}$. The small bands at around 600–700 cm$^{-1}$ are commonly related with out-of-plane C−C deformation vibrations and out-of-plane C−H bending, respectively, in monosubstituted aromatic rings [57]. In comparison to FTIR PANI spectrum (Fig. 1a), the fPANI FTIR spectrum (Fig. 2b) has characteristic band due to C=O group at 1688 cm$^{-1}$ for carboxylic acid [25,58]. As previously reported elsewhere [15,25,46], Fig. 2b of fPANI FTIR spectrum shows all key PANI peaks such as N−H stretching band, C−C stretching of quinoid and benzenoid bands, C=N band of imine group, electronic band of PANI and C−H out-of-plane bending in 1,4-disubstituted ring structures along with out-of-plane C−C deformation vibrations and out-of-plane C−H bending, respectively, in monosubstituted aromatic rings. However, in comparison with FTIR PANI spectrum (Fig. 2a), there is a shift in the peaks towards a slightly lower wavelength in FTIR spectrum of fPANI associated with N-H and to higher wavelength to the C−C stretching of quinoid peak and C=N band of imine group (Fig. 2b) which contributes due to presence of –COOH group.

After incorporation of Ag, PANI-Ag and fPANI-Ag FTIR spectra (Fig. 2c and d) show that the structural change of both colloids. FTIR spectrum of PANI-Ag colloid (Fig. 2c) displays a shift in the peaks toward a slightly lower or higher wavelength in comparison of PANI

associated C−C ring stretching, electronic band of PANI and the out-of-plane bending of the benzene ring, which indicates that the structural change of PANI polymer occurs after incorporation of Ag in PANI matrix. Furthermore, more profound changes are observed in FTIR spectrum of fPANI-Ag colloid with N−H stretching vibration shifted to higher wavelength, broadening and higher intensity in comparison to FTIR spectrum of fPANI (Fig. 2a), which suggests that Ag nanoparticles interacted with the nitrogen atom of the fPANI matrix [34,35]. In addition, the aromatic ring deformation peaks at 496 cm$^{-1}$ and 434 cm$^{-1}$ in fPANI FTIR spectrum (Fig. 2b) are shifted to lower wavelength in fPANI-Ag colloid (Fig. 2d), which indicate interactions between the Ag nanoparticles and aromatic rings present in the fPANI structure via incorporation of Ag nanoparticles into fPANI polymer [54].

*3.4. UV-Vis spectroscopy*

The UV–vis spectra of PANI and fPANI colloids were recorded to investigate their electronic properties and are presented in Fig. 3. UV-Vis spectrum of PANI showed the characteristic peaks at 290, 420 and the increasing absorbance toward the measuring limit of the instrument 800 nm (Stejskal and Sapurina reported an additional local maximum at the wavelength of 836 nm, [21]). These peaks are attributed to π→ π* transition of the benzenoid moieties in the polymer backbone, and polaron → π* and π→ polaron transitions, respectively are due to high conjugation of the aromatic PANI polymer chain [59,60]. In the case of UV-Vis spectrum of fPANI these peaks are slightly shifted due to presence of –COOH group in fPANI [25,58]. As previously reported by Dhivya et al. [9], the characteristic low wavelength polaron bands around 400–440 nm due to the conductive form of emeraldine salt form of PANI
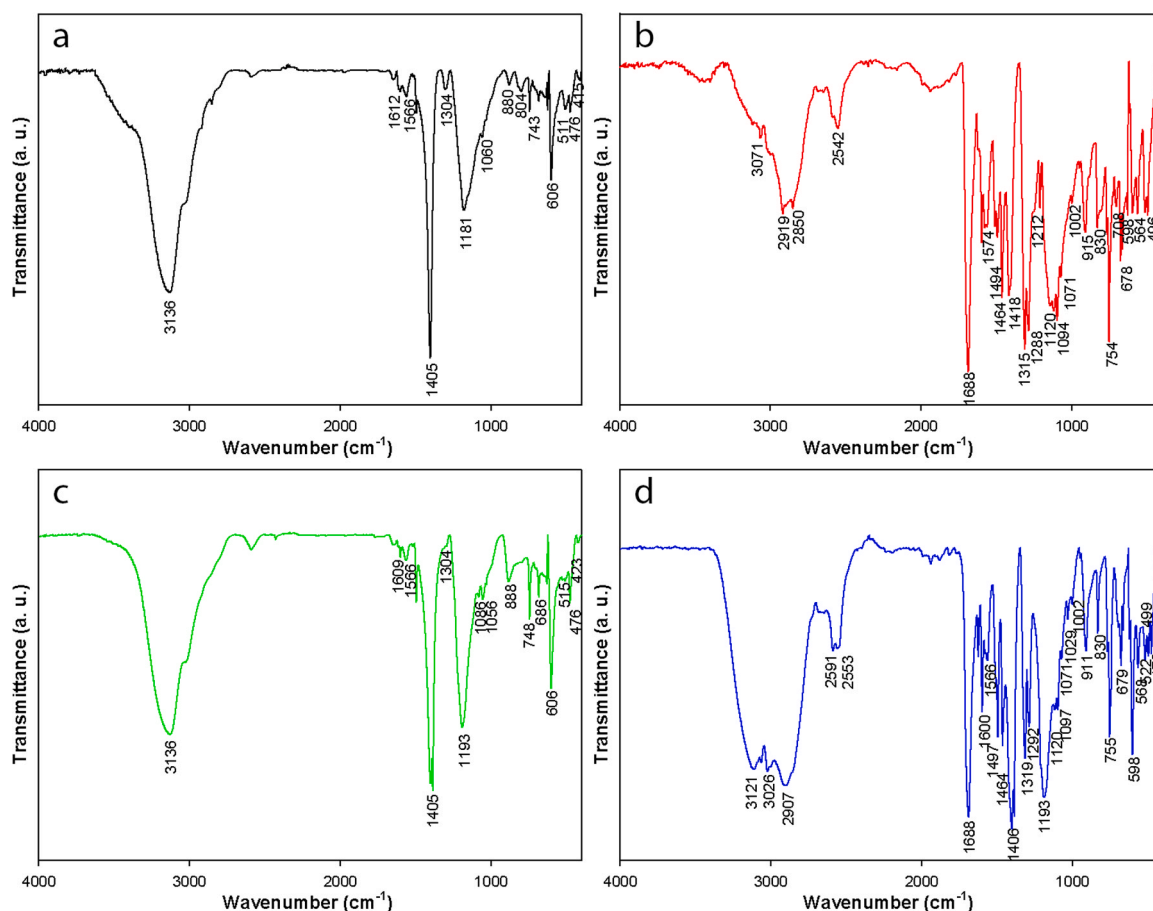


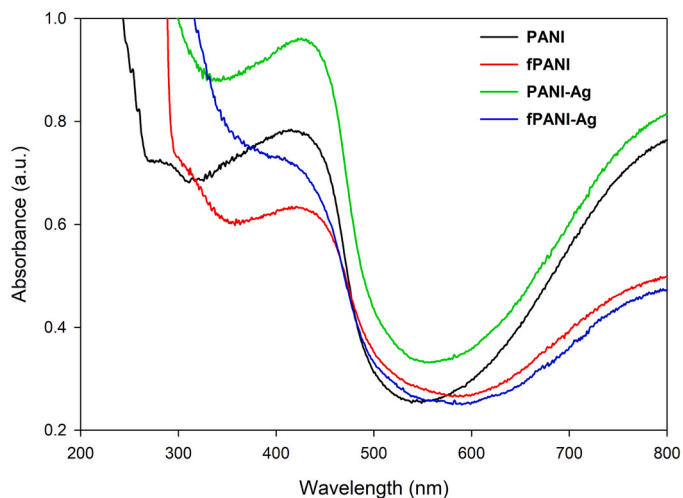**Fig. 2.** FTIR spectra of a) PANI, b) fPANI, c) PANI-Ag and d) fPANI-Ag.

**Fig. 3.** UV-Vis absorbance spectra of PANI and fPANI colloids.

based materials were observed in both PANI and fPANI colloids, along with the small free electron absorption tail in the region of 800–1100 nm.

In the UV-Vis spectrum of PANI-Ag two peaks due to polaron $\rightarrow \pi^*$ and $\pi \rightarrow$ polaron transitions shifted slightly to higher wavelengths [60]. These peaks undergo a hypsochromic shift in fPANI-Ag colloid because –COOH group disrupts the coplanarity of the $\pi^*$ system and obstructs charge delocalization [47]. The nature of the interactions between PANI and Ag nanoparticles, and the structural changes induced in the composite influence the shifts in absorbance peaks [61].

### 3.5. CV and EIS

EIS technique was employed to assess the charge transfer resistance and diffusion properties of the PANI, fPANI, and their Ag colloidal samples. As visualised from the Fig. 4, the Nyquist plot shows a smaller impedance arc and shorter low frequency tail for both PANI-Ag and fPANI-Ag compared to PANI and fPANI. The length of the arc is proportional to charge transfer resistance, while the low frequency tail indicates ion diffusion [62]. The Fig. 4 displays higher ion diffusion for films dispersed with PANI/fPANI-Ag colloids. This result indicates improved ion diffusion within the polymer matrix due to incorporation of Ag suggesting that this could facilitate the faster release of Ag ions into the polymer matrix indicating its higher antimicrobial efficacy. As per Fig. 4, the decrease in impedance arc indicates a high charge transfer
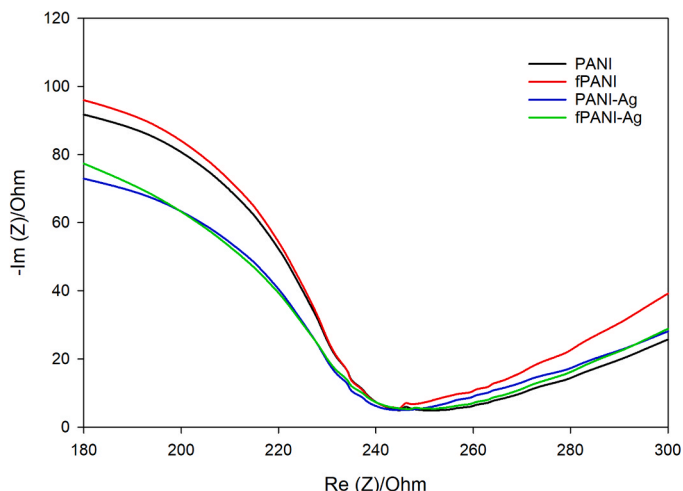
rate between the polymer chains. It can be observed that the impedance of PANI-Ag and fPANI-Ag is lower than PANI and fPANI. This shows the enhancement of conductivity of PANI with the addition of Ag. We speculate that this may be because the presence of Ag in the polymer matrix facilitates charge transfer between polymer chains, leading to less impedance. Therefore, the PANI/fPANI-Ag colloids can interact easily with microbial cells and disrupt their function, meaning higher antimicrobial activity [63].

The CV of the PANI, fPANI, and their PANI/fPANI-Ag colloids was examined to understand their electrochemical behaviour. While clear redox peaks are not visible, the CV plots of the samples provides insight into capacitive behaviour and stability of the PANI colloids. The results of the CV analysis further support the enhancement of conductivity for PANI-Ag and fPANI-Ag colloids (Fig. 5). Furthermore, since PANI is a pseudo capacitive material, all CV curves have a nonrectangular form, which suggests a faradic charge storage mechanism [64]. It can be noticed that the electrochemical activity observed for both PANI and fPANI samples are similar. Jokić et al. [60] reported that CV curve of fPANI contains two additional peaks in comparison to CV of PANI, which may be due to different mechanism of redox process [60,64–66]. However, no such characteristic peaks were observed for CV of fPANI in this study. In the case of PANI-Ag and fPANI-Ag samples, the slopes and intercepts of CV curves were greater than those of PANI and fPANI, which indicate that the incorporation of Ag nanoparticles had an impact on PANI and fPANI properties [64]. As previously reported, Ag nanoparticles can act as the conductive bridge between polymer chains resulting in an increase of conductivity of PANI composites [64]. Furthermore, the broad potential windows observed suggest that the materials remain electrochemically stable across various conditions, making them versatile for practical applications.

### 3.6. Evaluation of antibacterial and antiviral of properties of the colloids

The antimicrobial activity of the colloids was determined as MBC against *E. coli* and *S. aureus* and MVC against PhiX 174 (Table 2). Both PANI-Ag and fPANI-Ag colloids demonstrated enhanced bactericidal efficacy against Gram-negative *E. coli* and Gram-positive *S. aureus* bacteria in comparison to PANI and fPANI colloids. The fPANI-Ag colloid showed slightly better antiviral efficacy of 0.125 wt% against bacteriophage Phi X 174, than PANI-Ag. This result is in line with previously reported antiviral potency of fPANI polymers in contrast to PANI against Vaccinia virus [7]. Gizdavic-Nikolaidis et al. [7] reported that the number of Vaccinia virus which survived after 1 h of contact with 10 mg mL$^{-1}$ was 100% for PANI and none for fPANI.

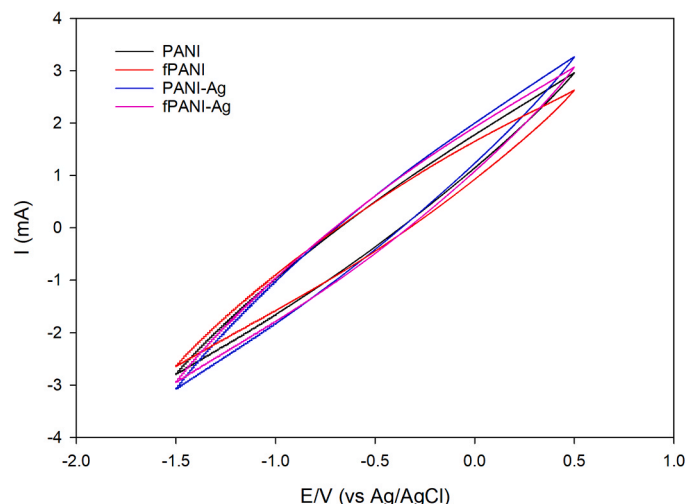The incorporation of Ag nanoparticles into the polymer matrix has



**Fig. 4.** Nyquist plot of PANI and fPANI colloids.



**Fig. 5.** CV of PANI and fPANI colloids.

**Table 2**
Antimicrobial results for PANI and fPANI colloids.

| Samples | MBC[*] for *E. coli* (wt%) | MBC[*] for *S. aureus* (wt%) | MVC[*] for *PhiX 174* (wt%) |
|---|---|---|---|
| PANI | 0.5 | 0.5 | 0.5 |
| fPANI | 0.5 | 0.5 | 0.25 |
| PANI-Ag | <0.0312 | 0.125 | 0.25 |
| fPANI-Ag | <0.0312 | 0.25 ± 0.125 | 0.125 |

[*] The MBC/MVC value is the median of three replicates. When the median values were different, the range is expressed (MBC/MVC ± range) and the others are expressed without ± range as all triplicates showed same value.

been established by FTIR, UV-Vis spectroscopy, CV and EIS studies. The inclusion of Ag in the PANI-Ag and fPANI-Ag colloids enhanced antimicrobial activity against *S. aureus* and bacteriophage Phi X 174 by 2–4-fold when compared to colloids of PANI and fPANI (Table 2). Moreover, the Ag-nanoparticles with Ag content (determined from ICP-MS study) matched to PANI-Ag and fPANI-Ag did not show antimicrobial activity (Table 1). PANI-Ag and fPANI-Ag colloid displayed activity at the highest dilution tested (0.0312 wt%) against *E. coli* indicating the improvement in antimicrobial activity of PANI and fPANI colloid. The increase in activity may be correlated to the increase in solubility (Fig. S1) and conductivity for PANI-Ag and fPANI-Ag indicated by the EIS spectra (Fig. 4). The results from conductivity studies reported by the authors exhibited that the electrical conductivity of PANI and fPANI increases with the incorporation of Ag nanoparticles [61]. Our research group has previously reported on the biocidal mechanism of PANI and fPANI [22,23,61,67]. It was observed that PANI and fPANI initiate dysregulation of microbial metabolism, leading to intracellular free radical production that accelerates cell death by damaging cellular components, such as proteins, lipids, and nucleic acids, ultimately impairing microbial viability [22,23,61,67]. In the case of fPANI, the presence of -COOH groups alters the redox reactions between the pathogen and pure PANI, thereby enhancing the production of free radicals [61,67]. Samples containing Ag exhibit a synergistic antimicrobial effect with PANI and fPANI [68]. Ag nanoparticles can induce electrochemical imbalance and are also absorbed into pathogenic cells, exerting activity from within the cell, facilitated by intracellular free radicals [68,69]. Therefore, the combination of fPANI with -COOH groups, which enhances the natural activity of fPANI along with Ag, demonstrates superior efficacy compared to PANI, fPANI and PANI-Ag samples (Table 2). The detailed elucidation of antibacterial and antiviral mechanism from experimental research is beyond the scope of the current study, but it will be studied in future.

Despite the limited number of Minimum Bactericidal Concentration (MBC) reports on PANI and PANI composites with both metals and non-metals [70–73], there is a notable absence of literature data regarding the MBC and Minimum Virucidal Concentration (MVC) values of PANI and PANI-Ag colloids. Therefore, direct comparisons of antimicrobial activity of PANI and PANI-Ag colloids against *E. coli*, *S. aureus* and bacteriophage from literature cannot be made. Additionally, there is a research gap concerning the antimicrobial activity of fPANI and fPANI-Ag colloids. PANI composites with noble metals (Au and Pt) exhibit promising antimicrobial activity against *E. coli*, albeit at potentially higher costs associated with material preparation [70,71]. Our study proposes an alternative cost-effective solution by introducing small amounts of Ag (10 mM) with PANI and fPANI. In addition, both PANI-Ag and fPANI-Ag performs better than PANI composites with non-metals [69]. Moreover, the activity of fPANI-Ag against *E. coli*, *S. aureus* and bacteriophage is not studied comprehensively in literature until date.

PANI composites with noble metals (Au and Pt) exhibit promising antimicrobial activity against *E. coli*, albeit at potentially higher costs associated with material preparation [70,71]. Our study proposes an alternative cost-effective solution by introducing small amounts of Ag (10 mM) with PANI and fPANI. In addition, both PANI-Ag and fPANI-Ag performs better than PANI composites with non-metals [69]. Moreover, the activity of fPANI-Ag against *E. coli*, *S. aureus* and bacteriophage has not been studied comprehensively in literature to date. Antimicrobial activity depends on a variety of surface properties of the colloidal particles. Improved activity may be due to higher dispersion, lower particle size and less impedance observed for PANI-Ag and fPANI-Ag colloids (Table 1). The investigated colloidal dispersions have aqueous-stable particle sizes in the range $10^2$ to $10^3$ nm, making them useful for a variety of applications where antibacterial and antiviral efficacy is required [15,19,22]. As previously reported, PANI and fPANI effectiveness against bacteria has been demonstrated [24,35], and Ag is recognized for antibacterial properties [25,35,47]. The improved activity seen with the combination of either PANI or fPANI with Ag maybe explained by the enhanced action of the two antimicrobial agents together. In addition, the smaller size and molecular weight of the particles may provide a greater surface area for action, improving activity [9,47,66].

## 4. Conclusions

In conclusion, this study successfully achieved a facile approach to create stable and active antimicrobial polyaniline (PANI) and carboxyl-functionalized polyaniline (fPANI) colloids. The introduction of -COOH functional groups in fPANI enhanced its processability compared to PANI. The addition of $AgNO_3$ to the fPANI system resulted in the development of a novel fPANI-Ag colloid, demonstrating high biocidal properties. The antimicrobial effectiveness of PANI and fPANI colloids was significantly improved by the inclusion of sub-lethal levels of Ag nanoparticles, incorporated through a one-pot synthesis approach. The integration of Ag nanoparticles into the polymer matrices led to reduced particle size, confirmed by structural and morphological analyses and enhanced solubility. Notably, the antimicrobial activity of fPANI-Ag is a novel contribution to the literature, and the study suggests that the enhanced properties may arise from the combination of PANI's conducting properties and Ag's catalytic and biocidal abilities. Moreover, the superior processability of fPANI-Ag positions it as a promising candidate for scaled-up production, particularly in diverse biomedical applications. Finally, the study provides promising suggestions for future research directions, such as enhancing synthesis parameters or assessing cytotoxicity, would strengthen the impact of this work.

**CRediT authorship contribution statement**

**Marija Gizdavic-Nikolaidis:** Writing – review & editing, Supervision, Formal analysis, Conceptualization. **Simon Swift:** Writing – review & editing, Validation, Supervision, Funding acquisition. **Darren Svirskis:** Writing – review & editing, Resources. **Mahima Bansal:** Writing – review & editing, Methodology. **Ajay Jose:** Writing – original draft, Investigation.

**Declaration of Competing Interest**

The authors declare the following financial interests/personal relationships which may be considered as potential competing interests: Simon Swift reports financial support was provided by University of Auckland. If there are other authors, they declare that they have no known competing financial interests or personal relationships that could have appeared to influence the work reported in this paper.

**Data availability**

Data will be made available on request.

## Acknowledgements

## Appendix A. Supporting information

Supplementary data associated with this article can be found in the online version at doi:10.1016/j.colsurfb.2024.113912.

## References

[1] A.A. Syed, M.K. Dinesan, Polyaniline - a novel polymeric material - review, Talanta 38 (1991) 815–837, https://doi.org/10.1016/0039-9140(91)80261-W.

[2] K. Shahin, L. Zhang, M.H. Mehraban, J.-M. Collard, A. Hedayatkhah, M. Mansoorianfar, A. Soleimani-Delfan, R. Wang, Clinical and experimental bacteriophage studies: Recommendations for possible approaches for standing against SARS-CoV-2, Microb. Pathog. 164 (2022) 105422, https://doi.org/10.1016/j.micpath.2022.105442.

[3] A. Jose, M. Gizdavic-Nikolaidis, S. Swift, Antimicrobial Coatings: Reviewing Options for Healthcare Applications, Appl. Microbiol. 3 (2023) 145–174, https://doi.org/10.3390/applmicrobiol3010012.

[4] F.V. Rheinbaben, S. Schünemann, T. Groß, M.H. Wolff, Transmission of viruses via contact in a household setting: experiments using bacteriophage φX174 as a model virus, J. Hosp. Infect. 46 (2000) 61–66. ⟨https://doi-org.ezproxy.auckland.ac.nz/10.1053/jhin.2000.0794⟩.

[5] R. Mao, X. Lv, M. Sui, T. Li, Inactivation of phage phiX174 by UV254 and free chlorine: structure impairment and function loss, J. Environ. Manag. 340 (2023) 117962, https://doi.org/10.1016/j.jenvman.2023.117962. ⟨https://doi-org.ezproxy.auckland.ac.nz/10.1016/j.jenvman.2023.117962⟩.

[6] N. Jarach, H. Dodiuk, S. Kenig, Polymers in the Medical Antiviral Front-Line, Polymers 12 (2020) 1727, https://doi.org/10.3390/polym12081727.

[7] M. Gizdavic-Nikolaidis, G. Bowmaker, Z. Zujovic. The Synthesis, Physical Properties, Bioactivity and Potential Applications of Polyanilines, first ed., Cambridge Scholars Publishing, UK, 2018.

[8] M. Gizdavic-Nikolaidis, J.Moreira Pupe, L.P. Silva, D. Stanisavljev, D. Svirskis, S. Swift, Composition tuning of scalable antibacterial polyaniline/chitosan composites through rapid enhanced microwave synthesis, J, Mat. Chem. Phys. 278 (2022) 125676, https://doi.org/10.1016/j.matchemphys.2021.125676.

[9] C. Dhivya, S.A.A. Vandarkuzhali, N. Radha, Antimicrobial activities of nanostructured polyanilines doped with aromatic nitro compounds, Arab. J. Chem. 12 (2019) 3785–3798, https://doi.org/10.1016/j.arabjc.2015.12.005.

[10] S.S. Pandey, S. Annapoorni, B.D. Malhotra, Synthesis and characterization of poly (aniline-co-o-anisidine). A processable conducting copolymer, Macromolecules 26 (1993) 3190–3193, https://doi.org/10.1021/ma00064a032.

[11] P.S. Rao, D.N. Sathyanarayana, Synthesis of electrically conducting copolymers of aniline with o/m-amino benzoic acid by an inverse emulsion pathway, Polymer 43 (2002) 5051–5058, https://doi.org/10.1016/S0032-3861(02)00341-5.

[12] A. Gök, B. Sarı, M. Talu, Synthesis and characterization of conducting substituted polyanilines, Synth. Met. 142 (2004) 41–48, https://doi.org/10.1016/j.synthmet.2003.07.002.

[13] J.Y. Bergeron, L.H. Dao, Electrical and physical properties of new electrically conducting quasi-composites. Poly(aniline-co-N-butylaniline) copolymers, Macromolecules 25 (1992) 3332–3337, https://doi.org/10.1021/ma00039a002.

[14] J. Guay, R. Paynter, L.H. Dao, Synthesis and characterization of poly (diarylamines): a new class of electrochromic conducting polymers, Macromolecules 23 (1990) 3598–3605, ⟨https://doi.org/10.1021/ma00217a010⟩.

[15] M.S. Lashkenari, H. Eisazadeh, Chemical copolymerization and characterization of colloidal Poly(aniline-co-3-aminobenzoic acid) as a high-Performance antibacterial polymer, Adv. Polym. Tech. 33 (2014), https://doi.org/10.1002/adv.21466.

[16] V. Kašpárková, D. Jasenská, Z. Capáková, N. Maráková, J. Stejskal, P. Bober, M. Lehocký, P. Humpolíček, Polyaniline colloids stabilized with bioactive polysaccharides: Non-cytotoxic antibacterial materials, Carbohydr. Polym. 219 (2019) 423–430, https://doi.org/10.1016/j.carbpol.2019.05.038.

[17] Z. Kucekova, P. Humpolíček, V. Kašpárková, T. Perecko, M. Lehocký, I. Hauerlandová, P. Sáha, J. Stejskal, Colloidal polyaniline dispersions: Antibacterial activity, cytotoxicity and neutrophil oxidative burst, Colloids Surf. B Biointerfaces 116 (2014) 411–417, https://doi.org/10.1016/j.colsurfb.2014.01.027.

[18] J. Huang, R.B. Kaner, Nanofiber formation in the chemical polymerization of aniline: A Mechanistic Study, Angew. Chem. 116 (2004) 5941–5945, https://doi.org/10.1002/anie.200460616.

[19] J.C.-C. Wu, S. Ray, M. Gizdavic-Nikolaidis, J. Jin, R.P. Cooney, Effect of polyvinylpyrrolidone on storage stability, anti-oxidative and anti-bacterial properties of colloidal polyaniline, Synth. Met. 217 (2016) 202–209, https://doi.org/10.1016/j.synthmet.2016.03.019.

[20] A. Riede, M. Helmstedt, V. Riede, J. Stejskal, Polyaniline dispersions. 9. Dynamic light scattering study of particle formation using different stabilizers, Langmuir 14 (1998) 6767–6771, https://doi.org/10.1021/la980365l.

[21] J. Stejskal, I. Sapurina, Polyaniline: Thin films and colloidal dispersions - (IUPAC technical report), Pure Appl. Chem. 77 (2005) 815–826, https://doi.org/10.1351/pac200577050815.

[22] M.R. Gizdavic-Nikolaidis, J.R. Bennett, S. Swift, A.J. Easteal, M. Ambrose, Broad spectrum antimicrobial activity of functionalized polyanilines, Acta Biomater. 7 (2011) 4204–4209, https://doi.org/10.1016/j.actbio.2011.07.018.

[23] J. Robertson, M. Gizdavic-Nikolaidis, S. Swift, Investigation of polyaniline and a functionalised derivative as antimicrobial additives to create contamination resistant surfaces, materials 11 (2018) 436, https://doi.org/10.3390/ma11030436.

[24] M.R. Gizdavic-Nikolaidis, S. Ray, J. Bennett, A.J. Easteal, R.P. Cooney, Electrospun functionalized polyaniline copolymer-based nanofibers with potential application in tissue engineering, Macromol. Biosci. 10 (2010) 1424–1431, https://doi.org/10.1002/mabi.201000237.

[25] M.R. Gizdavic-Nikolaidis, Z.D. Zujovic, S. Ray, A.J. Easteal, G.A. Bowmaker, Chemical synthesis and characterization of poly(aniline-co-ethyl 3-aminobenzoate) copolymers, J. Polym. Sci. Polym. Chem. A 48 (2010) 1339–1347, https://doi.org/10.1002/pola.23895.

[26] S. Bhattacharya, D. Kim, S. Gopal, A. Tice, K. Lang, J.S. Dordick, J.L. Plawsky, R. J. Linhardt, Antimicrobial effects of positively charged, conductive electrospun polymer fibers, Mat. Sci. Eng. C. 116 (2020) 111247, https://doi.org/10.1016/j.msec.2020.111247.

[27] Z. Kucekova, V. Kasparkova, P. Humpolicek, P. Sevcikova, J. Stejskal, Antibacterial properties of polyaniline-silver films, Chem. Pap. 67 (2013) 1103–1108, https://doi.org/10.2478/s11696-013-0385-x.

[28] M. Ghaffari-Moghaddam, H. Eslahi, Synthesis, characterization and antibacterial properties of a novel nanocomposite based on polyaniline/polyvinyl alcohol/Ag, Arab. J. Chem. 7 (2014) 846–855, https://doi.org/10.1016/j.arabjc.2013.11.011.

[29] A.A. Alhazime, K.A. Benthami, B.O. Alsobhi, G.W. Ali, S.A. Nouh, Pani-Ag/PVA nanocomposite: Gamma induced changes in the thermal and optical characteristics, J. Vinyl Addit. Techn. 27 (2020) 47–53, https://doi.org/10.1002/vnl.21782.

[30] F.M. Kelly, J.H. Johnston, T. Borrmann, M.J. Richardson, Functionalised hybrid materials of conducting polymers with individual fibres of cellulose, Eur. J. Inorg. Chem. 2007 (2007) 5571–5577, https://doi.org/10.1002/ejic.200700608.

[31] G. Nesher, M. Serror, D. Avnir, G. Marom, Silver coated vapor-grown-carbon nanofibers for effective reinforcement of polypropylene–polyaniline, Compos. Sci. Technol. 71 (2011) 152–159, https://doi.org/10.1016/j.compscitech.2010.11.005.

[32] M.S. Tamboli, M.V. Kulkarni, R.H. Patil, W.N. Gade, S.C. Navale, B.B. Kale, Nanowires of silver–polyaniline nanocomposite synthesized via in situ polymerization and its novel functionality as an antibacterial agent, Colloids Surf. B Biointerfaces 92 (2012) 35–41, https://doi.org/10.1016/j.colsurfb.2011.11.006.

[33] P. Boomi, H.G. Prabu, P. Manisankar, S. Ravikumar, Study on antibacterial activity of chemically synthesized PANI-Ag-Au nanocomposite, Appl. Surf. Sci. 300 (2014) 66–72, https://doi.org/10.1016/j.apsusc.2014.02.003.

[34] H. Zengin, G. Aksin, G. Zengin, M. Kahraman, I.H. Kilic, Preparation and characterization of conductive polyaniline/silver nanocomposite films and their antimicrobial studies, Polym. Eng. Sci. 59 (2019) E182–E194, https://doi.org/10.1002/pen.24902.

[35] M.R. Gizdavic-Nikolaidis, J.M. Pupe, A. Jose, L.P. Silva, D.R. Stanisavljev, D. Svirskis, S. Swift, Eco-friendly enhanced microwave synthesis of polyaniline/chitosan-AgNP composites, their physical characterisation and antibacterial properties, Synth. Met. 293 (2023) 117273, https://doi.org/10.1016/j.synthmet.2022.117273.

[36] J. Stejskal, M. Trchová, J. Kovářová, L. Brožová, J. Prokeš, The reduction of silver nitrate with various polyaniline salts to polyaniline–silver composites, React. Funct. Polym. 69 (2009) 86–90, https://doi.org/10.1016/j.reactfunctpolym.2008.11.004.

[37] L. Mulfinger, S.D. Solomon, M. Bahadory, A.V. Jeyarajasingam, S.A. Rutkowsky, C. Boritz, Synthesis and study of silver nanoparticles, J. Chem. Educ. 84 (2007) 322, https://doi.org/10.1021/ed084p322.

[38] H. Swaruparani, S. Basavaraja, A. Venkataraman, A new approach to solubility and processablity of polyaniline by poly(aniline-co-o-anisidine) conducting copolymers, Mat. Sci. Res. India 6 (2009) 335–342, https://doi.org/10.13005/msri/060212.

[39] D. Uppalapati, M. Sharma, Z. Aqrawe, F. Coutinho, I.D. Rupenthal, B.J. Boyd, J. Travas-Sejdic, D. Svirskis, Micelle directed chemical polymerization of polypyrrole particles for the electrically triggered release of dexamethasone base and dexamethasone phosphate, Inter. J. Pharm. 543 (2018) 38–45, https://doi.org/10.1016/j.ijpharm.2018.03.039.

[40] C. Yang, W. Dong, G. Cui, Y. Zhao, X. Shi, X. Xia, B. Tang, W. Wang, Enhanced photocatalytic activity of PANI/TiO2 due to their photosensitization-synergetic effect, Electrochim. Acta 247 (2017) 486–495, https://doi.org/10.1016/j.electacta.2017.07.037.

[41] Y. Guo, J. Nan, Y. Xu, F. Cui, W. Shi, Y. Zhu, Thermodynamic and dynamic dual regulation Bi2O2CO3/Bi5O7I enabling high-flux photogenerated charge migration for enhanced visible-light-driven photocatalysis, J. Mater. Chem. A 8 (2020) 10252–10259, https://doi.org/10.1016/j.electacta.2017.07.037.

[42] S. Wilschefski, M. Baxter, Inductively Coupled Plasma Mass Spectrometry: Introduction to analytical aspects, Clin. Biochem. Rev. 40 (2019) 115–133, https://doi.org/10.33176/aacb-19-00024.

[43] K. Yazaki, Electron microscopic studies of bacteriophage phi X174 intact and "eclipsing" particles, and the genome by the staining, and shadowing method, J. Virol. Methods 2 (1981) 159–167, https://doi.org/10.1016/0166-0934(81)90034-3.

[44] S. Sinha, S. Bhadra, D. Khastgir, Effect of dopant type on the properties of polyaniline, J. Appl. Polym. Sci. 112 (2009) 3135–3140, https://doi.org/10.1002/app.29708.

[45] J. Stejskal, P. Kratochvil, M. Helmstedt, Polyaniline dispersions. 5. Poly(vinyl alcohol) and poly(N-vinylpyrrolidone) as steric stabilizers, Langmuir 12 (1996) 3389–3392, https://doi.org/10.1021/la9506483.

[46] R.P. Singh, A. Tiwari, A.C. Pandey, Silver/polyaniline nanocomposite for the electrocatalytic hydrazine oxidation, J. Inorg. Organomet. Polym. 21 (2011) 788–792. ⟨https://doi.org/10.1007/s10904-011-9554-y⟩.

[47] N. Maráková, P. Humpolíček, V. Kašpárková, Z. Capáková, L. Martinková, P. Bober, M. Trchová, J. Stejskal, Antimicrobial activity and cytotoxicity of cotton fabric coated with conducting polymers, polyaniline or polypyrrole, and with deposited silver nanoparticles, Appl. Surf. Sci. 396 (2017) 169–176, https://doi.org/10.1016/j.apsusc.2016.11.024.

[48] D.W.O. de Medeiros, C.G. da Trindade Neto, D.E.S. dos Santos, F.J. Pavinatto, D. S. dos Santos, O.N. Oliveira Jr., A.E. Job, J.A. Giacometti, T.N.C. Dantas, M. R. Pereira, J.L.C. Fonseca, Preparation and Characterization of PAni-PMMA Dispersions, J. Dispers. Sci. Tech. 26 (2005) 267–273, https://doi.org/10.1081/DIS-200049560.

[49] C. Quintero-Quiroz, N. Acevedo, J. Zapata-Giraldo, L.E. Botero, J. Quintero, D. Zárate-Triviño, J. Saldarriaga, V.Z. Pérez, Optimization of silver nanoparticle synthesis by chemical reduction and evaluation of its antimicrobial and toxic activity, Biomater. Res 23 (2019) 27, https://doi.org/10.1186/s40824-019-0173-y.

[50] A. Bootz, V. Vogel, D. Schubert, J. Kreuter, Comparison of scanning electron microscopy, dynamic light scattering and analytical ultracentrifugation for the sizing of poly(butyl cyanoacrylate) nanoparticles, Eur. J. Pharm. Biopharm. 57 (2004) 369–375, https://doi.org/10.1016/S0939-6411(03)00193-0.

[51] K. Takayama, T. NAGAI, Application of interpolymer complexation of polyvinylpyrrolidone/carboxyvinyl polymer to control of drug release, Chem. Pharm. Bull. 35 (1987) 4921–4927, https://doi.org/10.1248/cpb.35.4921.

[52] S. Khairunnisa, V. Wonoputri, T.W. Samadhi, Effective deagglomeration in biosynthesized nanoparticles: a mini review, IOP Conf. Ser.: Mater. Sci. Eng. 1143 (2021) 012006, https://doi.org/10.1088/1757-899X/1143/1/012006.

[53] P. Bober, J. Stejskal, M. Trchová, J. Prokeš, In-situ prepared polyaniline–silver composites: Single- and two-step strategies, Electrochim. Acta 122 (2014) 259–266, https://doi.org/10.1016/j.electacta.2013.10.001.

[54] D.C. Pawar, D.B. Malavekar, S.D. Khot, A.G. Bagde, C.D. Lokhande, Performance of chemically synthesized polyaniline film based asymmetric supercapacitor: Effect of reaction bath temperature, Mat. Sci. Eng. B 292 (2023) 116432, https://doi.org/10.1016/j.mseb.2023.116432.

[55] M.R. Gizdavic-Nikolaidis, M. Jevremovic, D.R. Stanisavljev, Z.D. Zujovic, Enhanced Microwave Synthesis: Fine-Tuning of Polyaniline Polymerization, J. Phys. Chem. C. 116 (2012) 3235–3241, ⟨https://doi.org/10.1021/jp2086939⟩.

[56] M. Beygisangchin, S. Abdul Rashid, S. Shafie, A.R. Sadrolhosseini, H.N. Lim, Preparations, properties, and applications of polyaniline and polyaniline Thin Films—a review, Polymers 13 (2021) 2003, https://doi.org/10.3390/polym13122003.

[57] V. Kašpárková, D. Jasenská, Z. Capáková, N. Maráková, J. Stejskal, P. Bober, M. Lehocký, P. Humpolíček, Polyaniline colloids stabilized with bioactive polysaccharides: Non-cytotoxic antibacterial materials, Carbohydr. Polym. 219 (2019) 423–430, https://doi.org/10.1016/j.carbpol.2019.05.038.

[58] M. Gizdavic-Nikolaidis, D.R. Stanisavljev, A.J. Easteal, Z.D. Zujovic, Microwave assisted synthesis of functionalized polyaniline nanostructures with advanced antioxidant properties, J. Phys. Chem. C. 114 (2010) 18790–18796, https://doi.org/10.1021/jp106213m.

[59] R. Holze, Overoxidation of Intrinsically Conducting Polymers, Polymers 14 (2022) 1584, https://doi.org/10.3390/polym14081584.

[60] B.M. Jokić, E.S. Džunuzović, B.N. Grgur, B.Z. Jugović, T.L. Trišovic, J. S. Stevanović, M.M. Gvozdenović, The influence of m-aminobenzoic acid on electrochemical synthesis and behavior of poly(aniline-co-(m-aminobenzoic acid), J. Polym. Res. 24 (2017) 146, https://doi.org/10.1007/s10965-017-1313-5.

[61] A. Jose, P. Yadav, D. Svirskis, S. Swift, M.R. Gizdavic-Nikolaidis, Antimicrobial photocatalytic PANI based-composites for biomedical applications, Synth. Met. 303 (2024) 117562, https://doi.org/10.1016/j.synthmet.2024.117562.

[62] A. Jose, S.D.K.R. Pai, D. Pinheiro, K. Kasinathan, Visible light photodegradation of organic dyes using electrochemically synthesized $MoO_3$/ZnO, Env. Sci. Pollut. Res. 28 (2021) 52202–52215, https://doi.org/10.1007/s11356-021-14311-9.

[63] J. Li, G. Wang, H. Zhu, M. Zhang, X. Zheng, X. Liu, X. Wang, Antibacterial activity of large-area monolayer graphene film manipulated by charge transfer, Sci. Rep. 4 (2014) 4359, https://doi.org/10.1038/srep04359.

[64] M. Khesuoe, M. Matoetoe, F. Okumu, Potential of Silver Nanoparticles Functionalized Polyaniline as an Electrochemical Transducer, J. Nano Res. 44 (2016) 21–34. ⟨https://doi.org/10.4028/www.scientific.net/JNanoR.44.21⟩.

[65] R. Gangopadhyay, A. De, Conducting polymer nanocomposites: A brief overview, Chem. Mater. 12 (2000) 608–622, https://doi.org/10.1021/cm990537f.

[66] L.L. Wang, L.Q. Shao, The antimicrobial activity of nanoparticles: present situation and prospects for the future, Inter. J. Med. 12 (2017) 1227–1249, https://doi.org/10.2147/IJN.S121956.

[67] J. Robertson, M. Gizdavic-Nikolaidis, M.K. Nieuwoudt, S. Swift, The antimicrobial action of polyaniline involves production of oxidative stress while functionalisation of polyaniline introduces additional mechanisms, Article e5135, PeerJ 6 (2018), https://doi.org/10.7717/peerj.5135.

[68] Q. Jia, S. Shan, L. Jiang, Y. Wang, D. Li, Synergistic antimicrobial effects of polyaniline combined with silver nanoparticles, J. Appl. Polym. Sci. 125 (2012) 3560–3566, https://doi.org/10.1002/app.36257.

[69] E.O. Mikhailova, Silver nanoparticles: mechanism of action and probable bio-Application, J. Funct. Biomater. 11 (2020) 84, https://doi.org/10.3390/jfb11040084.

[70] P. Boomi, H. Gurumallesh Prabu, Synthesis, characterization and antibacterial analysis of polyaniline/Au–Pd nanocomposite, Colloid Surf. A Physicochem. Eng. Asp. 429 (2013) 51–59, https://doi.org/10.1016/j.colsurfa.2013.03.053.

[71] P. Boomi, H.G. Prabu, J. Mathiyarasu, Synthesis, characterization and antibacterial activity of polyaniline/Pt–Pd nanocomposite, Eur. J. Med. Chem. 72 (2014) 18–25, https://doi.org/10.1016/j.ejmech.2013.09.049.

[72] W. Cai, J. Wang, X. Quan, X., Z. Wang, Preparation of bromo-substituted polyaniline with excellent antibacterial activity, J. Appl. Polym. Sci. 135 (2018) 45657, https://doi.org/10.1002/app.45657.

[73] A. Janošević Ležaić, I. Pašti, A. Gledović, J. Antić-Stanković, D. Božić, S. Uskoković-Marković, G. Ćirić-Marjanović, Copolymerization of aniline and gallic acid: Novel electroactive materials with antioxidant and antimicrobial activities, Synth. Met 286 (2022) 117048. ⟨https://doi.org/10.1016/j.synthmet.2022.117048⟩.